Journal of Fluids and Structures 42 (2013) 358–368

Contents lists available at ScienceDirect

Journal of Fluids and Structures

journal homepage: www.elsevier.com/locate/jfs

Influence of slip on vortex-induced motion of a superhydrophobic cylinder

Robert Daniello, Pranesh Muralidhar, Nicholas Carron, Mark Greene, Jonathan P. Rothstein*

Department of Mechanical and Industrial Engineering, University of Massachusetts—Amherst, Amherst, MA 01003, USA

ARTICLE INFO

Article history:
Received 30 July 2012
Accepted 22 April 2013
Available online 13 August 2013

Keywords:
Superhydrophobic
Ultrahydrophobic
Superhydrophobicity
Slip
Partial slip
Drag reduction
Vortex
Cylinder

ABSTRACT

The partial slip boundary condition produced by a superhydrophobic surface in the Cassie state has been shown capable of reducing skin friction drag as well as influencing the flow around coated bodies including cylinders and spheres. In this paper, we investigated how the changes in vortex shedding and separation previously observed on superhydrophobic cylinders affects the rms lift force and the resulting oscillations induced on an elastically mounted cylinder. Two hydrophobic polytetrafluoroethylene cylinders were studied. The first was smooth and the second was roughened to make it superhydrophobic and to induce slip. The presence of slip was found to decrease rms lift and amplitude of the oscillating cylinder by up to 15% with no measurable impact on drag or the natural frequency of the elastically mounted system. We show that the observed reductions are a direct result of reduced fluid forcing on the superhydrophobic cylinder.

1. Introduction

The use of superhydrophobic surfaces to create a partial slip boundary condition has been established in the literature and shown to result in drag reduction in both laminar (Cottin-Bizonne et al., 2003; Choi and Kim, 2006; Ou et al., 2004; Ybert et al., 2007) and turbulent flows (Balasubramanian et al., 2004; Daniello et al., 2009; Gogte et al., 2005; Henoch et al., 2006). Superhydrophobic surfaces combine chemical hydrophobicity with microscale surface structure to produce a composite solid/gas/liquid boundary. They were originally observed in the water repellency of many plant and insect species (Bush et al., 2008; Shirtcliffe et al., 2009), the most famous example being the self-cleaning lotus leaf (Barthlott and Neinhuis, 1997). While such surfaces appear rough, the micro- or nanometer-sized surface features combine with the high contact angles resulting from the chemical hydrophobicity of the material to prevent water from moving into the space between the peaks of the surface. As a result, an air–water interface is formed between the microfeatures as illustrated by the schematic diagram in Fig. 1. There is no single defining characteristic for microstructure or roughness necessary for a surface to exhibit superhydrophobic behavior. It may be random or ordered, isotropic or directional and it may be composed of one or several (hierarchical) lengthscales. The resulting surface exposes less solid area to wetting, despite its apparent roughness, and the presence of the resulting fluid–vapor interface with the trapped gas produces the observed partial slip condition.

* Corresponding author. Tel.: +1 413 577 0110.
E-mail address: rothstein@ecs.umass.edu (J.P. Rothstein).

0889-9746/$ - see front matter
http://dx.doi.org/10.1016/j.jfluidstructs.2013.04.006

Drag reduction has been observed on streamlined bodies with a superhydrophobic coating (Balasubramanian et al., 2004; Gogte et al., 2005; McHale et al., 2009); however, the effects resulting from the partial slip boundary condition are not limited to a reduction in friction drag. Simulations of You and Moin (2007) and Legendre et al. (2009) demonstrated that adding slip at the surface of a cylinder in crossflow affects the resulting lift, separation and vortex intensity in the cylinder's wake. Legendre et al. (2009) used direct numerical simulations, DNS with arbitrary uniformly applied partial slip boundary conditions to investigate flow past a cylinder over a range of modified Knudsen numbers ($\mathrm{Kn}=b/R=$slip length/radius). Their simulations predict a delayed onset of shedding with increasing slip length and an extended steady separated wake. At large Knudsen numbers, the slip length reaches a value large enough that fluid advection downstream outstrips vorticity generation at the surface of the cylinder (from curving streamlines as well as from shear when $\mathrm{Kn}<\infty$) resulting in an unseparated wake at all Reynolds numbers. Unfortunately, the observed wake stabilization requires Knudsen numbers too large for experimental observation on a macroscale cylinder with the 20–200 μm slip lengths observed from superhydrophobic surfaces (Rothstein, 2010). Even at smaller, yet still experimentally feasible, slip lengths, Legendre et al. (2009) predict increased vortex shedding frequency in the presence of slip along with reduced vortex intensity in the wake and rms lift. Experiments of Muralidhar et al. (2011) observed the predicted increase in shedding frequency with slip in the flow direction created from superhydrophobic coated cylinders. Additionally, the authors observed delayed onset of shedding and elongation in the recirculation region in the presence of superhydrophobic surfaces along with notable changes in separation point with sensitivity to slip direction. When superhydrophobic microridges, and hence the slip direction, ran circumferentially the separation point advanced towards the leading edge of the cylinder while reorienting the microfeatures along the length of the cylinder produced the opposite effect. Conversely, enabling slip axially along the length of the cylinder was observed to reduce vortex shedding frequency. Vortex shedding results in cyclic fluctuations of lift force experienced by the cylinder, which are capable of exciting periodic oscillations in the case of an elastically-mounted cylinder. Presently, we seek to investigate how the addition of a partial slip boundary condition affects the rms lift force and the resulting self-exciting motions of a cylinder.

Vortex-induced vibrations (VIV) occur when pressure fluctuations accompanying vortex shedding excite motion in an elastic or elastically mounted body. This is shown schematically in Fig. 2. These usually undesirable vibrations can be especially destructive to long slender structures such as oil risers, mooring lines, bridges, chimneys, pipes, cables, heat exchanger tubes and many similar applications. Like vortex shedding, VIV has been the subject of generations of research stretching back to Rayleigh's (1879) observations on vibrating harp strings. More recently, reviews by Bearman (1984) and Williamson and Govardhan (2004) and many texts such as those of Blevins (2001) and Sumer and Fredsøe (1997) have been

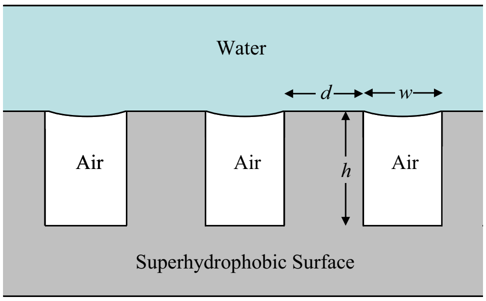

Fig. 1. Schematic diagram of air trapped between hydrophobic microfeatures of a superhydrophobic surface. The air–water interface produces shear free regions resulting in a reduction in wetted area and regions that can experience significant slip in flows.

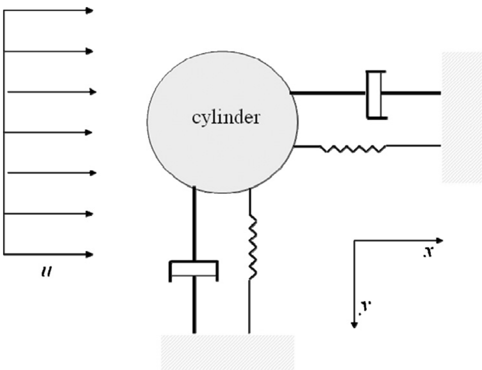

Fig. 2. Schematic of the spring mass (cylinder) dashpot system used to model vortex induced vibrations.

written on the phenomenon. Unlike vortex shedding from a rigid cylinder, VIV is determined by the interaction of fluid dynamics and the motion of the elastic body. On an elastically mounted cylinder initially at rest, shedding begins to occur as in the stationary case, until the periodic impulses from the shed vortices approach a natural frequency of the body. This assumes, of course, that the rigidity and natural frequency lie within the range where VIV will occur. As the body begins to move, its movement in turn affects the frequency of the shedding, synchronizing the behavior along the spanwise length of the cylinder and giving the cylinder the ability to affect the shedding frequency (Bearman, 1984). The synchronization of shedding and natural frequencies is termed lock-in; it brings high oscillation amplitudes at nearly constant frequency that persists over a wide range of Reynolds numbers. The onset of oscillations has been shown to increase vortex strength, alter phase and pattern of vortices in the wake and increase drag on the cylinder by a factor of two or more (Blevins, 2001). In this paper, we experimentally study how a partial slip boundary condition affects vortex-induced vibrations.

2. Experimental set-up

It has previously been observed that polytetrafluoroethylene (PTFE) can be used to fabricate an excellent superhydrophobic surface if proper microfeatures can be imparted onto its surface using abrasives of various grits (Nilsson et al., 2010). Micrographs of these sanded PTFE surfaces can be seen in Fig. 3. The jagged surface of the abraded material creates a multiscale surface which has proven effective for enhancing drop mobility (Nilsson et al., 2010). Observations on vortex shedding of static cylinders demonstrated that orienting slip direction with that of the bulk flow resulted in vortex elongation, greater separation and reduced swirling strength. To maximize this effect on the oscillating cylinders, PTFE blanks prepared from commercial Teflon hollow rod (MSC, Melville NY), were roughened circumferentially in a lathe by first lightly scribing with a ganged stack of razors and subsequently with 240 grit sandpaper. The resulting surface was found to perform well, exhibiting substantial shear free area apparent by the visible plastron (McHale et al., 2009) on the submerged cylinder. Observable superhydrophobicity persisted when left submerged for several days. Additionally, the very high percentage of shear free area likely negated microfeature orientation as continuous shear free paths were observable in all directions. In contrast, the microstructured PDMS surfaces of Muralidhar et al. (2011) stationary shedding experiments would exhibit 50% shear free area under ideal conditions and continuous shear free paths 15 μm or 30 μm wide separated by ridge tops of no slip having equal width.

Elastically mounted cylinder experiments were conducted by suspending the horizontal cylinder from extension springs affixed to its ends by slender nichrome wires centered within the test section of the water tunnel (Engineering Laboratory Design, Model 501). The springs were situated above the water level. A schematic of the set-up is shown in Fig. 4. The oscillatory behavior of the experiments necessitated precisely weighted cylinders of identical length and end conditions, accomplished by filling center with cylindrical lead weights cast from a custom mold. After weight matching, the weights were slid into the cylinder flush with both ends of the tube, producing a solid perpendicular end. PDMS surfaces were not utilized in the present experiments as their fabrication technique produces larger weight variations and necessitates a seam. The suspending wire was inserted between the tube and the weights so that it extended from the top on both ends of the cylinder. Weights of the completed cylinders were found to match within 0.5%. All cylinders had $D = 9.8$ mm with an aspect ratio of $\ell/D = 16$.

Morse et al. (2008) considered the effects of end conditions on the response of an oscillating elastically mounted cylinder and determined a gap greater than 15% between the cylinder and endplate was equivalent to a free end, while gaps below 15% were equivalent to an endplate attached to the cylinder. Surprisingly, there was no change in peak amplitude related to the presence of the endplate and the high amplitude oscillations were found to more steady without the endplate, but with

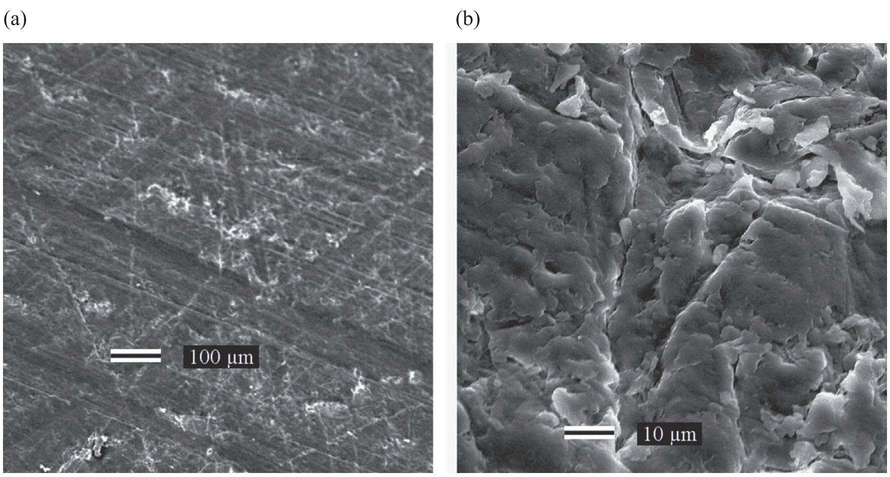

Fig. 3. SEM images of PTFE surfaces sanded with 240 grit sandpaper, (a) at 100 × and (b) at 1000 × , showing the microscale roughness imparted to the surface.

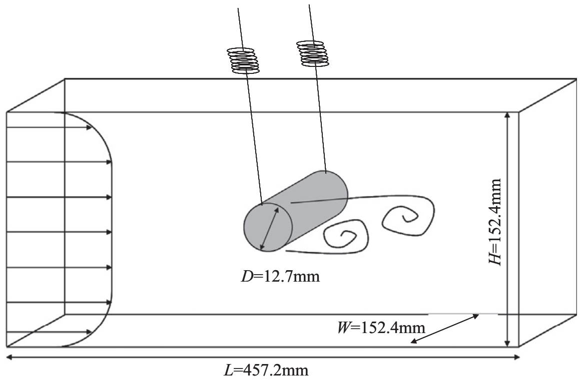

Fig. 4. Schematic diagram of flow cell. Both smooth cylinders and cylinders coated with superhydrophobic surfaces were tested.

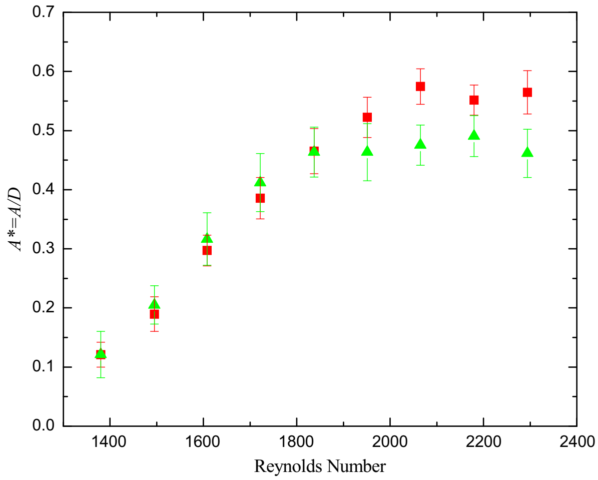

Fig. 5. Reduced amplitude, $A^*=A/D$, of cylinder oscillations over a range of Reynolds numbers corresponding to $4.2<U^*<7.1$ for superhydrophobic coated (▲) and no-slip (■) cylinders. Vortex induced vibrations amplitude reductions of 15% are observed. Peak amplitude occurs at Re=2065 and $U^*=5.7$.

a loss of clear distinction between the upper and lower branch modes of oscillation (Morse et al., 2008). For the present experiments, no endplates were used and cylinder end gaps being 30% of cylinder diameter, due in part to practical considerations surrounding the suspending wires and small cylinder diameters, the present experiments do not seek to investigate mode transition In all cases, cylinder length and end spacing were maintained consistently across all experiments. Particle image velocimetry (PIV) was utilized to examine the wake structure. Additionally, the cylinder motion was tracked by a Phantom (Phantom V.2) high-speed camera focused on the end of the cylinder. Cylinder motions were tracked with the OpenCV template matching plug-in utility in ImageJ. Oscillation frequency was calculated using a fast Fourier transform and average amplitude was determined by a local peak finder (and also alternatively from Fourier coefficients). Flow velocity was determined from the previously calibrated settings on the water tunnel. Experiments were conducted with at least four repetitions on several unique smooth and superhydrophobic cylinders over Reynolds numbers between $1300<\mathrm{Re}=UD/\nu<2300$. In all flow cases oscillations were flow induced.

3. Results and discussion

3.1. Oscillating cylinders

Previous studies have achieved VIV amplitude reductions with boundary layer modifications such as the experiments of Korkischko and Meneghini (2012) who utilized a moving wall to inject momentum into the boundary layer around the cylinder, decreasing velocity fluctuations, oscillation amplitude and drag on the cylinder. Partial slip boundary conditions, such as those that are physically realizable through the use of superhydrophobic surfaces, have been shown to reduce vortex strength and lift on the stationary cylinder in simulations of You and Moin (2007) and Legendre et al. (2009). It is expected that a reduced lift coefficient would correspond with reduced fluid forcing and therefore lower amplitude oscillations in the y direction normal to the flow direction (in x). In Fig. 5 the amplitude ratio, $A^*=A/D$, is presented for a range of Reynolds numbers corresponding to reduced velocities between $4.2 < U^* = U/f_N D < 7.1$ on PTFE cylinders. Here A is the amplitude of cylinder oscillations, D is the diameter of the cylinder, U is the flow velocity and f_N is the natural frequency of the system. Under certain conditions, amplitude reductions up to 15% are observed with the superhydrophobic coating, with the greatest reduction occurring at the maximum oscillation around a reduced velocity of $U^* = 5.7$. To investigate repeatability, experiments were repeated with multiple unique cylinders. The data in Fig. 5 represents up to fourteen individual experiments.

Free decay of forced oscillations were examined to determine what role if any, slip plays in the fluid damping of a cylinder undergoing oscillations. These experiments were conducted with the cylinders in the water tunnel in otherwise motionless water. Set-up, cylinders and springs were those previously used in elastically mounted cylinder experiments. Cylinders were displaced and released, the subsequent oscillations being tracked and recorded as with the flow induced case. Resulting oscillations and decay are shown in Fig. 6. Decay rate was determined by fitting a decaying exponential of this data which is overlaid on the decaying oscillatory motion of the cylinder in Fig. 6. The decay exponent showed no perceptible correlation between slip and decay rate; oscillations decayed at equal rate with or without the presence of the superhydrophobic coating. The frequency of the freely decaying oscillations calculated to be 4.03 Hz for both the smooth and superhydrophobic cylinder. Additionally, the damping ratio, $\zeta = c/2\sqrt{k(m+m_A)}$, which can be calculated directly from the decay experiments (Khalak and Williamson, 1999) showed the both system to have the same relatively high structural damping, $\zeta = 0.038$. Here c and k are the damping and spring coefficients of the system, respectively, m is the mass of the cylinder and m_A is the added mass. Equivalent decay rate indicates that the reduced amplitudes observed with the presence of a slip surface are the result of reduced fluid forcing and not by affecting fluid damping on the oscillating cylinder. It is therefore not surprising that the vortex induced oscillation frequency appears unaffected by the presence of slip, as shown in Fig. 7.

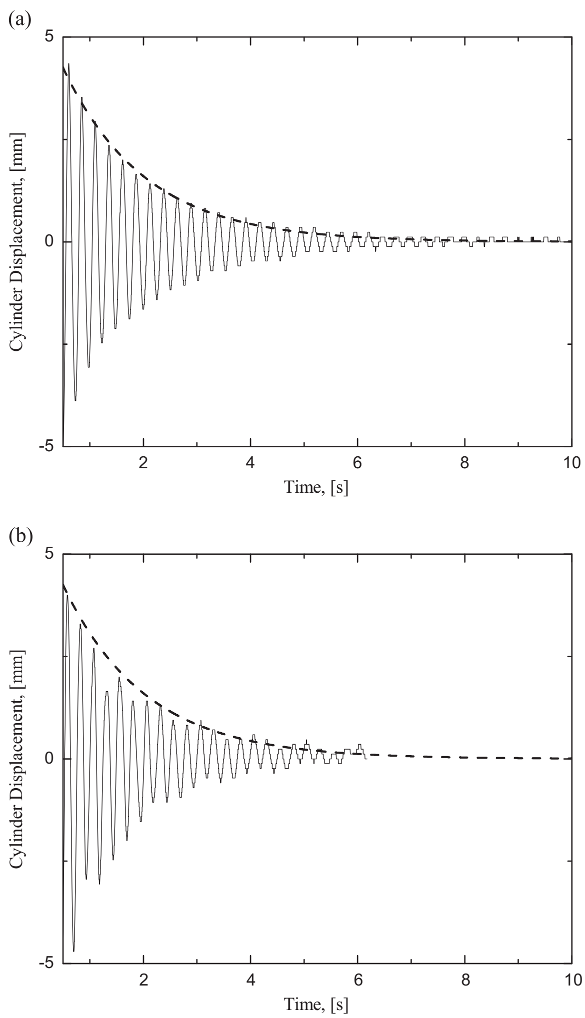

Fig. 6. Decay of oscillations from a forced cylinder in still water. Shown is the measured free decay (–) superhydrophobic (a), and smooth no-slip (b) along with identical decaying exponential fits plotted on top of the data (‒).

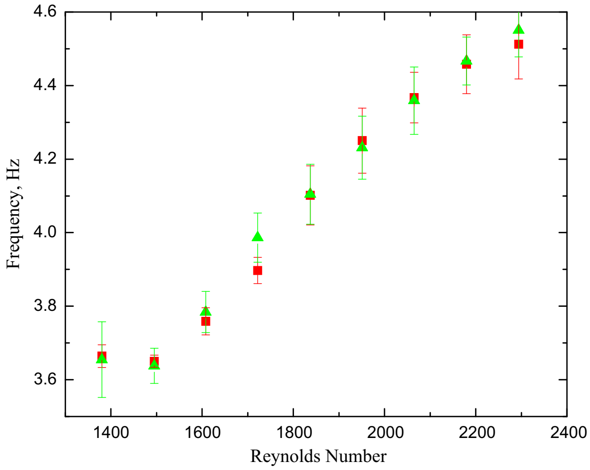

Fig. 7. Frequency of vortex induced oscillations for superhydrophobic PTFE (▲) and smooth no-slip PTFE (■) cylinders.

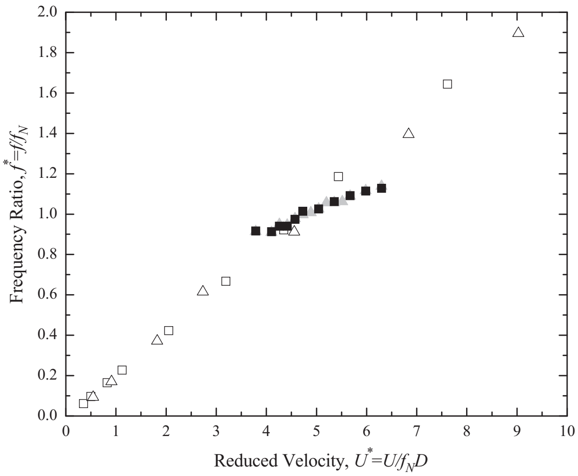

Fig. 8. Vortex shedding and lock-in for superhydrophobic and no-slip PTFE cylinders. Stationary no-slip cylinder (□), stationary superhydrophobic PTFE cylinder (△), oscillating no-slip cylinder (■) and oscillating superhydrophobic PTFE cylinder (▲).

The use of lead weights in the present cylinders results in a mass ratio, $m^*=m/m_A=4.8$, for experiments being conducted in water. The resulting $m^*\zeta=0.18$ mass-damping parameter is high, but not unprecedented for experiments conducted in water (generally at much higher Reynolds number) (Khalak and Williamson, 1999). The low Reynolds number experiments of Anagnostopoulos and Bearman (1992) conducted at $m^*\zeta=0.179$ showed a maximum oscillation amplitude ratio of $A^*=0.55$. In the present experiments, the maximum amplitude ratio observed for the no-slip cylinders at nearly identical mass-damping is seen to be in very good agreement at $A^*=0.57$. Similar maximum amplitudes ratios are seen for outside of low mass-damping. Bearman (1984) and Khalak and Williamson (1999) point out that for high mass ratio cylinders, that is those much more dense than the fluid they displace, the frequency at which the cylinder will oscillate, and thus the natural frequency of the system, are very close to that of shedding from the stationary cylinder, resulting in a frequency ratio near unity. Fig. 8 shows the lock-in behavior of elastically mounted smooth and superhydrophobic cylinders plotted along with shedding from the analogous stationary cylinders. Resonance occurs around the observed natural frequency of the system ($f_N=4.03$ Hz), just after the onset of oscillations, shedding frequencies of the stationary and oscillating cylinders match at a Reynolds number around Re≈1700, corresponding to a reduced velocity of $U^*\approx4.4$ for the no-slip smooth PTFE cylinder. The result is lock-in over a range corresponding to reduced velocities between $5<U^*<7$ over a wide span of Reynolds numbers. It can be seen that despite the expected increase in shedding frequencies that accompanies slip at the surface once the cylinder begins oscillating ($f^*\approx1$) the natural frequency of the structure becomes dominant in lock-in and the frequency of oscillations is independent of the presence of slip. It is also expected that if anything, the higher slip-cylinder shedding frequency would approach the natural frequency of the cylinder sooner, inducing the onset of oscillations at a lower Reynolds number, as even with its delayed onset in the presence of slip, shedding occurs nearly a decade before the onset of oscillations. Unfortunately, the present set-up lacks the low end resolution for such a study.

3.2. Stationary cylinders—lift and drag measurements

In order to better compare stationary shedding measurements with the present PTFE cylinders, the static shedding measurements were performed on a rigid PTFE cylinder fabricated in the same manner as those used for the elastic case. PIV observations of the wake confirm that the superhydrophobic PTFE cylinders demonstrate the same trends observed by Muralidhar et al. (2011) for flow-oriented PDMS cylinders. Specifically, the roughened PTFE cylinders shed a more widely separated, higher frequency vortex street with elongated vortices and lower vortex intensity. PIV conducted on oscillating cylinders confirms these trends persist qualitatively as the cylinder is allowed to oscillate. Vorticies were identified using the swirling strength criterion of Zhou et al. (1999), the imaginary part of the complex eigenvalue pair (λ_{ci}), as eigenvalues are only complex in the presence of swirling motion, swirling strength distinguishes vortices from irrotational but with non-zero vorticity (Chakraborty et al., 2005). Fig. 9 shows swirling strength behind oscillating smooth and superhydrophobic PTFE cylinders averaged over many shedding cycles (3.3 and 5 s). Without slip, vortices are seen to follow two separated paths behind the cylinder, with vorticity of opposing sign. In all cases, the presence of slip reduced the organization of the clearly defined, separate tracks of vortex motion observed from the no-slip cylinders. As a result, a narrower region of low vorticity directly behind the cylinder and often a wider wake were observed in the presence of slip. Fig. 10 shows snap-shots of vector fields in the wake of oscillating microstructured PTFE cylinder overlaid with the z-component of vorticity.

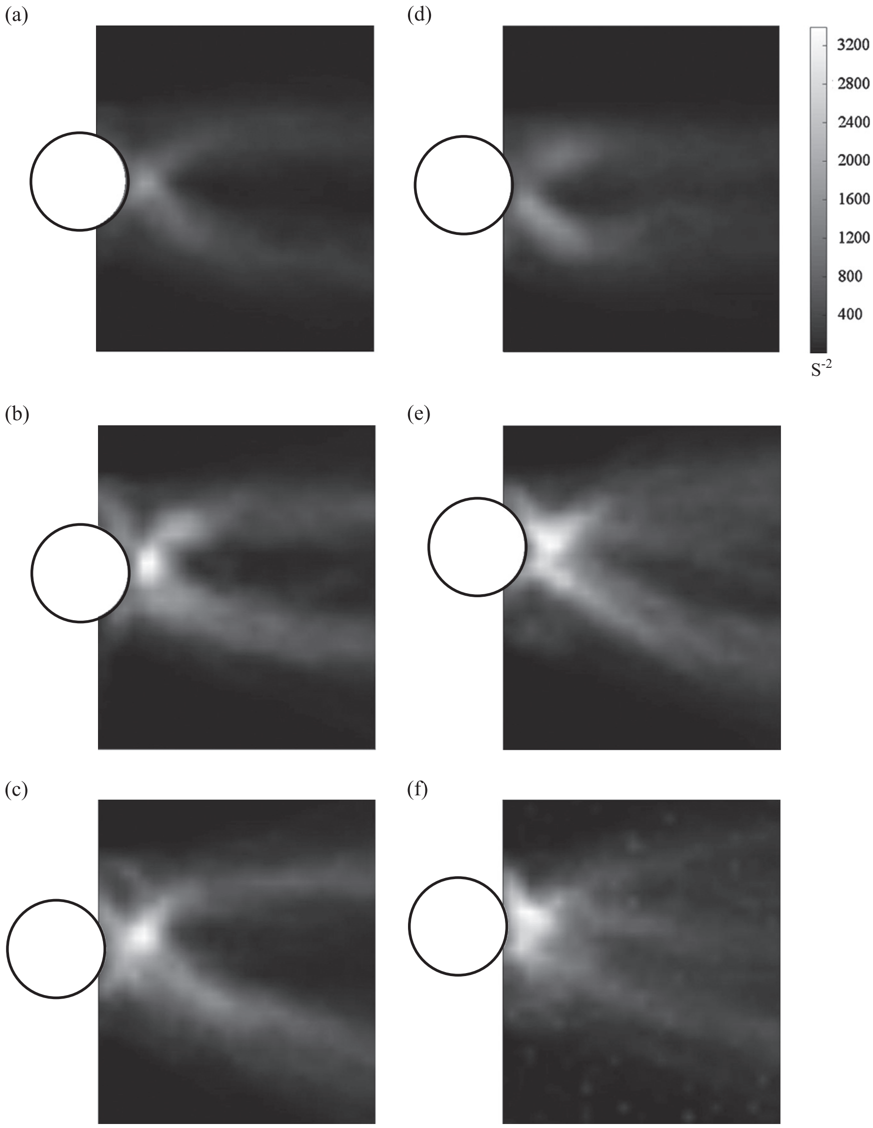

Fig. 9. Time averaged swirling strength for no-slip (left) and superhydrophobic coated (right) PTFE cylinders: (a) no-slip Re = 2065, 3.3 s of data; (b) no-slip Re = 1950, 3.3 s of data; (c) no-slip Re = 1840, 5 s of data; (d) superhydrophobic coated Re = 2065, 3.3 s of data; (e) superhydrophobic coated Re = 1950, 3.3 s of data and (f) superhydrophobic coated Re = 1840, 5 s of data.

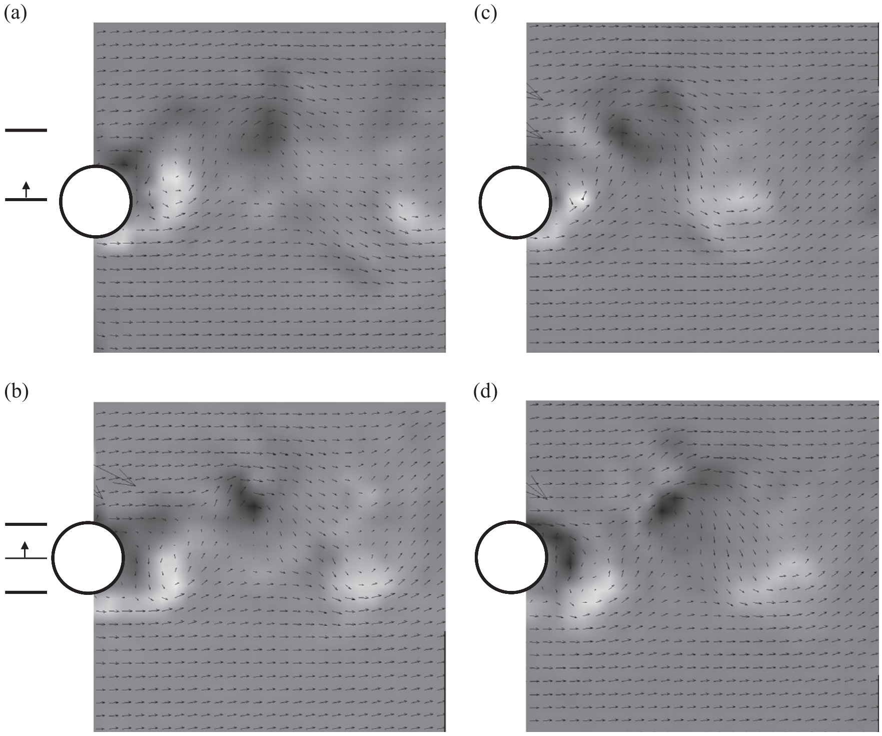

Fig. 10. PIV vector fields behind an oscillating cylinder with smooth surface (a, b) (left) and with Teflon PTFE surface (c, d) (right) at Re = 1840. The cylinder is at its lowest point in (a) and (b), and is at the centerline traveling upward in (c) and (d).

Wider separation of vortices, less interlacing and greater disorder in the wake are evident in the wake of the slip cylinder. It should be noted that for the superhydrophobic slip case presented on the right side of Fig. 10, vortices move much farther from the center as compared to the no slip case on the left side of Fig. 10. The resulting structure of the oscillating cylinder's wake is qualitatively similar to the increased separations and reduced interlacing observations from the corresponding stationary cylinders. These changes in vortex shedding dynamics can have a significant impact on the magnitude of lift forces exerted on the stationary or oscillating cylinder.

Investigations of the lift and drag coefficients were performed on the stationary PTFE cylinders. The lift force on a cylinder in crossflow oscillates with time as vortices are shed with alternating positive and negative vorticity. The mean lift force on the cylinder is zero, as a result, to characterize the strength of the lift force on a cylinder the root mean square (rms) value of the lift force is often used, $F_{L,rms}$. A lift coefficient can be defined from the rms lift force as

$$C_{L,rms} = \frac{F_{L,rms}}{\frac{1}{2}\rho U^2 DL}. \tag{1}$$

Here ρ is the density of water, U is the free-stream velocity, D is the cylinder diameter and L is the spanwise length of the cylinder exposed to flow. There is a wide spread in the value of the rms lift coefficients in the literature (Norberg, 2003), extending from $C_{L,rms}=0.1$–0.2 for 3-D spanwise averaged lift measurements to O(1) values for 2-D (single-plane) measurements. On a stationary cylinder, vortices shed at different phases along the length of the cylinder, out of phase contributions partially canceling, hence the force measured by a transducer (which is a spanwise averaged measurement) is significantly less than that which would be obtained from a 2-D sectional measurement. 3-D lift or drag measurements are typically obtained through direct measurement of lift or drag force using force transducers. Conversely, 2-D lift or drag measurements are made using velocimetry or pressure tap measurements that focus on a single plane in the wake of the cylinder and cannot resolve variations in the flow along the length of the cylinder. Thus, although 2-D measurements cannot predict an absolute value of lift or drag, they can be used as a comparative tool to determine relative differences in lift between a smooth no-slip cylinder and a superhydrophobic slip cylinder. On cylinder subject to VIV in the lock-in region, cylinder motion controls vortex shedding which occurs simultaneously along the length of the oscillating cylinder. As a result, in the lock-in region, parallel shedding behavior makes 2-D lift measurements more appropriate for comparison than 3-D lift measurements taken on a stationary cylinder.

In the current experiments, 3-D drag measurement showed no measurable difference between the slip and the no-slip cylinder. This is not surprising given that at these relatively small values of the Knudsen number, the predictions of Legendre et al. (2009) predict less than a 5% drag reduction. Legendre et al. (2009) do, however, predict a slightly larger reduction on lift. Unfortunately, due to the extremely small alternating lift forces for our current experiments, 3-D measurements of lift were not possible and it was necessary to probe the wake of the cylinder using PIV. From these detailed measurements of the velocity field and the vortex shedding dynamics, an estimate of the lift force at the mid-section of the cylinder can be calculated. The technique involves calculating the time rate of change of vorticity in the wake of the cylinder and the unsteady fluid dynamic forces on the cylinder using the impulse concept, first explained by Lamb (1945). The impulse concept states that the lift force on the cylinder is equal and opposite to the force which the cylinder exerts on the flow to produce the oscillating flow patterns. Lighthill (1986) showed that Lamb's impulse concept could be used to calculate force acting on the cylinder as the time rate of change of the moment of vorticity around the cylinder. For a 2-D flow, the lift force reduces to (Lin and Rockwell, 1996; Noca et al., 1997):

$$L=\rho\frac{\mathrm{d}}{\mathrm{d}t}\int_A x\omega_z\,\mathrm{d}A. \tag{2}$$

Here ω_z is the vorticity in the z-plane and dA is composed of piecewise area elements of the 2-D control volume chosen from the PIV data.

A number of groups have used these non-intrusive techniques to measure lift because, as described above, the oscillating lift force from the cylinder is often below the transducer resolution. Lin and Rockwell (1996) used the time variation of spatial vorticity packets in the wake of the cylinder to estimate the fluid dynamic forces acting on an oscillating cylinder in otherwise quiescent water. In their study, the cylinder was started up from rest and only a few cycles were observed so as to confine all of the vorticity to the region in the wake of the cylinder they could interrogate with PIV. This was done because the impulse method requires the time evolution of all the shed vortices to give an accurate force estimation value. This can only be achieved if the domain is large enough that the vortices decay before they reach the edge or, for the case of a start-up flow, if the vorticity is confined within a finite domain. Lin and Rockwell (1996) found good agreement of the lift coefficient estimated by the impulse method with the measured value over the course of 1.5 shedding cycles. Later, Noca et al. (1997) set out to compute the lift force acting on a cylinder using vorticity data from an arbitrary, finite control volume surrounding the body. Noca et al. (1997) showed that the impulse method could be extended to finite control volumes if the flux of vorticity out of the control volume is taken into account. Noca's modified version of the impulse equation is given as

$$-\mathbf{F}_{ext}=-\frac{1}{N-1}\frac{\mathrm{d}}{\mathrm{d}t}\int \boldsymbol{x}\wedge\omega\mathrm{d}V+\oint_S\hat{\boldsymbol{n}}\cdot\boldsymbol{\tau_i}\,\mathrm{d}S, \tag{3}$$

where $\mathbf{F}_{ext}$ is the force on the cylinder, N is the dimension, $\hat{\mathbf{n}}$ is the unit normal to surface S, $\boldsymbol{\omega}$ and $\boldsymbol{u}$ are vorticity and velocity and tensor $\boldsymbol{\tau_i}$ is given by

$$\boldsymbol{\tau_i}=\frac{1}{2}u^2\boldsymbol{I}-\boldsymbol{uu}-\frac{1}{N-1}\boldsymbol{u}(\boldsymbol{x}\wedge\omega)+\frac{1}{N-1}\omega(\boldsymbol{x}\wedge\boldsymbol{u}). \tag{4}$$

The validity of this velocimetry technique for determining the fluid forces on a bluff body was confirmed by Tan et al. (2005) through a series of 2-D simulations of a no-slip cylinder in crossflow. Through numerical simulations they were able to directly compare the forces evaluated from the velocity fields using Eq. (3) to the forces obtained by integration of the pressure and viscous stresses around the cylinder. Their simulations showed good agreement.

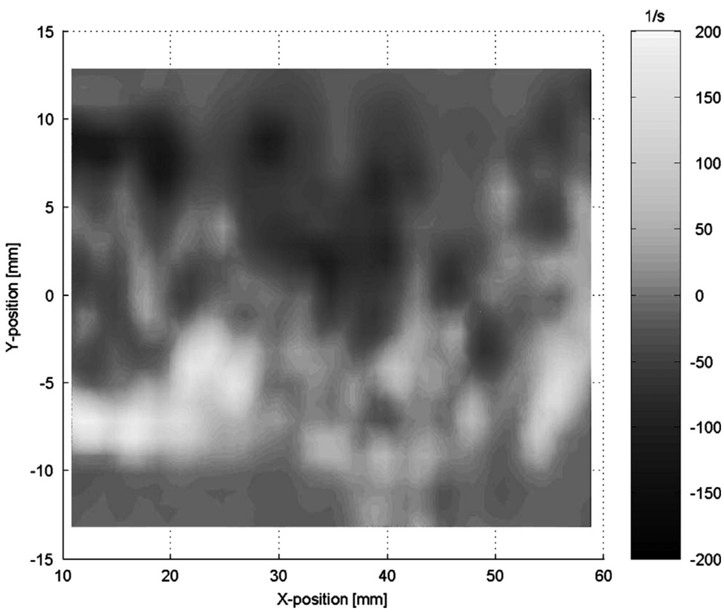

Fig. 11. Contours showing vorticity in the wake of a smooth circular cylinder at a Reynolds number of Re=4160. The center of the cylinder (not shown in the figure) lies at $X=Y=0$.

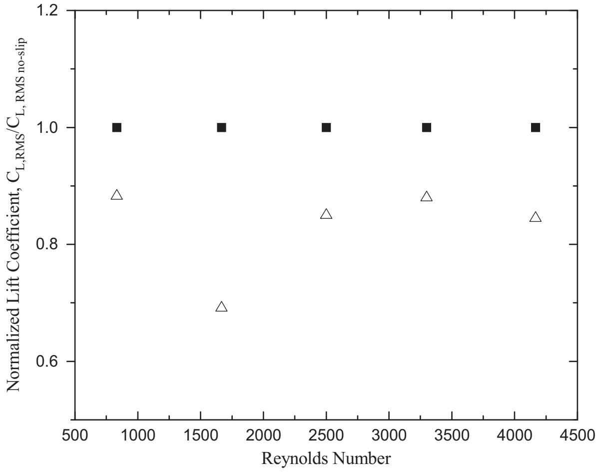

Fig. 12. Normalized lift coefficient, $C_{L,rms}/C_{L,rms\ No\text{-}slip}$, as a function of Reynolds number showing that superhydrophobic cylinders produce less rms lift compared to smooth cylinders. The data include: smooth cylinder (■), and a superhydrophobic cylinder produced by sanding a Teflon cylinder (Δ).

In the present experiments, lift force on a stationary cylinder was performed using Noca's (1997) technique. To arrive at the lift coefficients of the no slip and two different superhydrophobic slip cylinders, 2-D PIV measurements, $N=2$, were performed at the mid-section of the cylinders and the velocity vectors were computed using a commercial PIV code (DaVis, LaVision Gmbh). The illumination of the PIV particles is provided by a laser light sheet passed across the cross section of the cylinder. The region above the cylinder is therefore in shadow; the control volume was chosen extending from immediately behind the cylinder to approximately five cylinder diameters downstream. A time series of spatial vorticity fields was computed from the velocity data using a circulation estimate (Raffel et al., 2007). An example of a vorticity snapshot is shown in Fig. 11 for the no-slip cylinder at a Reynolds number of Re=4160. Vortices shed from the smooth cylinder are found to be more coherent and more tightly interlaced with each other than those shed from the slip cylinder. To determine the lift force as a function of time, Eq. (4) was applied to the control volume in Fig. 11. The resulting time varying lift coefficients can be used to calculate an rms lift coefficient. In Fig. 12, the rms lift coefficients obtained for a smooth and 240 grit sanded PTFE cylinder are presented non-dimensionalized relative to the no-slip cylinder to better understand the effect that slip has on lift. From Fig. 12, it is evident that the sanded PTFE superhydrophobic surface reduces the rms lift coefficient by approximately 15–20%. The lift reduction is approximately independent of Reynolds number over this range. The magnitude of the reduction in the lift coefficient agrees well with the predictions of Legendre et al. (2009), whose results, conducted for Re≤800 observe an increased sensitivity to slip with increasing Reynolds number. Additionally, these reductions are in good agreement with the 15% amplitude reductions observed on the oscillating cylinders, lift coefficient being proportional to the fluid forcing term affected by slip on the oscillating cylinders. Thus it appears clear that the reduction in amplitude of oscillation for the superhydrophobic cylinder is a direct result of a reduction in the rms lift generated by slip along the surface of the circular cylinder.

4. Conclusions

In this work, a series of experiments were performed to investigate the influence of slip on the flow past a circular cylinder. The partial slip boundary condition was produced by coating the circular cylinder with a series of superhydrophobic, randomly patterned surfaces formed by roughening PTFE. When compared with smooth cylinders, the presence of slip on a cylinder was found to increase the length and width of the recirculation region in the wake of a superhydrophobic coated cylinder while decreasing its lift coefficient and the intensity of the shed vortices. When allowed to oscillate, slip was shown to decrease the amplitude of oscillatory motion without affecting the natural frequency of the system. Oscillation decay experiments showed no difference as a result of slip, indicating that the amplitude reduction was a result of reduced fluid forcing. Lower rms lift coefficients were confirmed by non-intrusive lift measurements on stationary cylinders. The partial slip condition does not appear to affect fluid damping of the oscillating cylinder. This work demonstrated experimentally that slip at the surface of circular cylinder can have a strong impact on the vortex shedding dynamics and rms lift force of a cylinder in crossflow.

Acknowledgments

The authors would like to thank NSF for funding this research under Grant CBET-0967531.

References

Anagnostopoulos, P., Bearman, P.W., 1992. Response characteristics of a vortex-excited cylinder at low Reynolds-numbers. Journal of Fluids and Structures 6, 39–50.
Balasubramanian, A.K., Miller, A.C., Rediniotis, O.K., 2004. Microstructured hydrophobic skin for hydrodynamic drag reduction. AIAA Journal 42, 411–414.
Barthlott, W., Neinhuis, C., 1997. Purity of the sacred lotus, or escape from contamination in biological surfaces. Planta 202, 1–8.
Bearman, P.W., 1984. Vortex shedding from oscillating bluff bodies. Annual Review of Fluid Mechanics 16, 195–222.
Blevins, R.D., 2001. Flow-Induced Vibration. Krieger Publishing Company, Malabar, FL.
Bush, J.W.M., Hu, D.L., Prakash, M., 2008. The integument of water-walking arthropods: form and function. Advances in Insect Physiology 34, 117–192.
Chakraborty, P., Balachandar, S., Adrian, R.J., 2005. On the relationships between local vortex identification schemes. Journal of Fluid Mechanics 535, 189–214.
Choi, C.H., Kim, C.J., 2006. Large slip of aqueous liquid flow over a nanoengineered superhydrophobic surface. Physical Review Letters 96 (066001), 1–4.
Cottin-Bizonne, C., Barrat, J.-L., Bocquet, L., Charlaix, E., 2003. Low-friction flows of liquid at nanopatterned interfaces. Nature Materials 2, 237–240.
Daniello, R., Waterhouse, N.E., Rothstein, J.P., 2009. Turbulent drag reduction using superhydrophobic surfaces. Physics of Fluids 21 (085103), 1–9.
Gogte, S., Vorobieff, P., Truesdell, R., Mammoli, A., van Swol, F., Shah, P., Brinker, C.J., 2005. Effective slip on textured superhydrophobic surfaces. Physics of Fluids 17 (051701), 1–4.
Henoch, C., Krupenkin, T.N., Kolodner, P., Taylor, J.A., Hodes, M.S., Lyons, A.M., Peguero, C., Breuer, K., 2006. Turbulent drag reduction using superhydrophobic surfaces. In: Collection of Technical Papers—3rd AIAA Flow Control Conference, vol. 2, pp. 840–844.
Khalak, A., Williamson, C.H.K., 1999. Motions, forces and mode transitions in vortex-induced vibrations at low mass-damping. Journal of Fluids and Structures 13, 813–851.
Korkischko, I., Meneghini, J.R., 2012. Suppression of vortex-induced vibration using moving surface boundary-layer control. Journal of Fluids and Structures 34, 259–270.
Lamb, S.H., 1945. Hydrodynamics. Dover Publications.
Legendre, D., Lauga, E., Magnaudet, J., 2009. Influence of slip on the dynamics of two-dimensional wakes. Journal of Fluid Mechanics 633, 437–447.
Lighthill, J., 1986. Fundamentals concerning wave loading on offshore structures. Journal of Fluid Mechanics 173, 667–681.
Lin, J.-C., Rockwell, D., 1996. Force identification by vorticity fields: techniques based on flow imaging. Journal Fluids and Structures 10, 663–668.
McHale, G., Shirtcliffe, N.J., Evans, C.R., Newton, M.I., 2009. Terminal velocity and drag reduction measurements on superhydrophobic spheres. Applied Physics Letters 94 (064104), 1–3.
Morse, T.L., Govardhan, R.N., Williamson, C.H.K., 2008. The effect of end conditions on the vortex-induced vibration of cylinders. Journal Fluids and Structures 24, 1227–1239.
Muralidhar, P., Ferrer, N., Daniello, R., Rothstein, J.P., 2011. The influence of slip on the flow past superhydrophobic circular cylinders. Journal of Fluid Mechanics 680, 459–476.
Nilsson, M.A., Daniello, R.J., Rothstein, J.P., 2010. A novel and inexpensive technique for creating superhydrophobic surfaces using teflon and sandpaper. Journal of Physics D: Applied Physics 43 (045301), 1–5.
Noca, F., Shiels, D., Jeon, D., 1997. Measuring instantaneous fluid dynamic forces on bodies, using only velocity fields and their derivatives. Journal of Fluids and Structures 11, 345–350.
Norberg, C., 2003. Fluctuating lift on a circular cylinder: review and new measurements. Journal of Fluids and Structures 17, 57–96.
Ou, J., Perot, B., Rothstein, J.P., 2004. Laminar drag reduction in microchannels using ultrahydrophobic surfaces. Physics of Fluids 16, 4635–4643.
Raffel, M., Willert, C.E., Wereley, S.T., Kompenhans, J., 2007. Particle Image Velocimetry: A Practical Guide. Springer.
Rayleigh, L., 1879. Acoustical observations. Philosophical Magazine S 5, 149–162.
Rothstein, J.P., 2010. Slip on superhydrophobic surfaces. Annual Review of Fluid Mechanics 42, 89–109.
Shirtcliffe, N.J., McHale, G., Newton, M.I., 2009. Learning from superhydrophobic plants: the use of hydrophilic areas on superhydrophobic surfaces for droplet control. Langmuir 25, 14121–14128.
Sumer, B.M., Fredsøe, J., 1997. Hydrodynamics around Circular Structures. World Scientific Publishing, Singapore.
Tan, B.T., Thompson, M.C., Hourigan, K., 2005. Evaluating fluid forces on bluff bodies using partial velocity data. Journal of Fluids and Structures 20, 5–24.
Williamson, C.H.K., Govardhan, R., 2004. Vortex-induced vibrations. Annual Review of Fluid Mechanics 36, 413–455.
Ybert, C., Barentin, C., Cottin-Bizonne, C., Joseph, P., Bocquet, L., 2007. Achieving large slip with superhydrophobic surfaces: scaling laws for generic geometries. Physics of Fluids 19, 123601.
You, D., Moin, P., 2007. Effects of hydrophobic surfaces on the drag and lift of a circular cylinder. Physics of Fluids 19, 081701.
Zhou, J., Adrian, R.J., Balachandar, S., Kendall, T.M., 1999. Mechanisms for generating coherent packets of hairpin vortices in channel flow. Journal of Fluid Mechechanics 387, 353–396.